Effect of using Klobuchar, CODE, and No-Ionosphere Models on Processing Single Frequency GPS Static Medium Baselines

Khaled Mohamed Abdel Mageed

Abstract - The ionospheric delay, which is affecting GPS measurements, is frequency dependant, that is the lower the frequency, the greater the delay. Generally, the ionospheric delay is of the order of 5 m, but it can reach over 15m under extreme solar activities, at midday and high altitudes. GPS dual frequency receivers can combine L1 and L2 carrier phase measurements to generate ionosphere-free linear combination to remove ionospheric delay, but has some disadvantages. For single frequency receivers, the empirical ionospheric models such as Klobuchar can correct up to 60% of the delay; or corrections from regional or global IGS networks such as CODE can be received in real time through communication links.

This paper investigates the effect of using Klobuchar model, CODE correction model, or in case of not using any ionosphere model, on the accuracy of the resulted Cartesian coordinates of processing GPS medium baselines up to 40km, using static technique and single frequency data L1. The results supported by statistical analysis showed that the positional discrepancies between Klobuchar model and no-ionosphere has a mean value of 14.6mm and 5.4mm standard deviation; while the positional discrepancy between CODE model and no-ionosphere model has a mean value of 16.8mm with 6.0mm standard deviation. In addition, the positional discrepancy between Klobuchar and CODE models has a mean value of 6.6mm with 2.0mm standard deviation, which means that both Klobuchar and CODE models are giving almost the same results. These findings may be adopted for establishing first order geodetic networks up to 40km baseline lengths with less-expensive GPS single frequency receivers; as well as it is recommended to use the same ionosphere model in processing GPS data for monitoring of structure deformation to maintain mm accuracy.

Index Terms - GPS, Ionosphere Delay, Klobuchar Model, CODE Ionosphere Corrections, IGS

1. Introduction

There are many sources of possible errors that are degrading the accuracy of positions computed by GPS receivers. The travel time of GPS satellite signals can be altered by atmospheric effects; when a GPS signal passes through the ionosphere and troposphere it is refracted, causing the speed of the signal to be different from the speed of a GPS signal in space; in addition to the sunspot activity which also causes interference with GPS signals [1]. Another source of error is measurement noise, or distortion of the signal caused by electrical interference or errors inherent in the GPS receiver itself. Errors in the ephemeris data which are transmitted via navigation message and contain information about satellite orbits will also cause errors in computed positions, due to some force fields, which are affecting their motion. Small variations in the atomic clocks or clock drift on board the satellites can translate to large position errors. Multipath effect arises when signals transmitted from the satellites bounce off a reflective surface before getting to the receiver antenna. When this happens, the receiver gets the signal in straight line path as well as delayed or multiple paths [2].

• *Khaled Abdel Mageed: Associate Professor of Civil Engineering, Higher Technological Institute, HTI, Egypt. E-mail: Khaled_mgd@yahoo.com.*

The atmosphere region where gas ionization takes place is called ionosphere. This region extends from an altitude of approximately 50 km to about 1000 km, or more. In fact, the upper limit of the ionospheric region in not clearly defined. The electron density within the ionospheric region is not constant, because it changes with altitude. Based on this fact, the ionospheric region is divided into layers, according to electron density [3]. These layers are named D, which ranges from 50-90 km; E, which ranges from 90 to 140 km; F1, which ranges from 140-210 km; and finally F2, which is usually being the layer of maximum electron density. The altitude and thickness of these layers are varying with time, as a result of the change in the sun's radiation and earth's magnetic field [4].

The ionosphere error is considered as the most important error source due to its high values, and for this reason its contribution has to be corrected. Ignoring the treatment of this error makes cycle slip editing and ambiguity resolution more difficult, and also introduces scale errors especially for long baselines. Consequently, in case of not treating of this error, it is recommend to take GPS Observations at night if possible, where ionospheric activity is minimized at night [5].

This paper investigates the effect of using Klobuchar, CODE global ionosphere model; or not using any ionosphere model on the resulted Cartesian X, Y, and Z, coordinates and the spatial positional accuracy P; for GPS medium baselines up to 40km proceeded by Static technique . The characteristics of the ionosphere delay will be introduced. Klobuchar model will be presented along with its mathematical model. Different available global ionosphere models as well as agencies that are providing these services will be summarized. The methodology of investigation and the description of the field test will be presented. Finally, the analysis of the obtained results supported with the statistical analysis will be shown, from which the important conclusions and recommendations will be concluded.

2. Characteristics of Ionosphere Delay

The ionospheric delay is frequency dependant, that is, the lower the frequency, the greater the delay. Consequently, L2 ionospheric delay is greater than that of L1. Generally, the ionospheric delay is of the order of 5 m to 15 m, but it can reach over 150m under extreme solar activities, at midday and near horizon [6]. Ionosphere delay can be determined with a high degree of accuracy by combining the P-code pseudorange measurements on both L1 and L2. Differencing the GPS observations between receivers of short separation can remove the major part of the ionospheric delay. Dual frequency receivers can combine L1 and L2 carrier phase measurements to generate ionosphere-free linear combination to remove ionospheric delay [7]. This is one of the main advantages of dual frequency receivers. Disadvantages of the ionosphere-free linear combination are: a relatively higher observation noise; does not preserve the integer nature of the ambiguity parameters; and is not recommended for short baselines. Single frequency users cannot take advantage of the dispersive nature of the ionosphere. However, they may use one of the empirical ionospheric models to correct up to 60% of the delay [8]. Klobuchar model is one of the most widely used models whose coefficients are transmitted as part of the navigation message. Alternatively, single frequency GPS users can use corrections from regional or global networks such as International GNSS Service IGS stations [9]. Such corrections can be received in real time through communication links.

There are two types of GPS observables, namely the code pseudoranges and carrier phase observables. In general, the pseudorange observations are used for coarse navigation, whereas the carrier phase observations are used in high precision surveying applications. This is due to the fact that the accuracy of the carrier phase observations is much higher than the accuracy of code observations [10]. The general form of code pseudorange observation equation is:

$$P = \rho + C(dt - dT) + \Delta^{iono} + \Delta^{Trop} + d_{orb} + \varepsilon_p \quad (1)$$

Where: P is the observed pseudorange; ρ is the unknown geometric satellite to receiver range; C is speed of light; dt and dT are satellite and receiver clock errors respectively; Δ^{iono}, Δ^{Trop}, are the error due to ionospheric, tropospheric refraction respectively, d_{orb} is the orbital error andε_p is the code measurement noise. The observation equation of the phase pseudorange is:

$$\emptyset = \rho + C(dt - dT) + \lambda N - \Delta^{iono} + \Delta^{Trop} + d_{orb} + \varepsilon_\phi \quad (2)$$

Where, the measured phase is indicated in meters by Φ, λ is the carrier wavelength, N is the phase ambiguity, and ε_ϕ is the phase noise, and the other remaining symbols are the same as defined in equation (1).

Ionosphere speeds up the propagation of the carrier phase, while it slows down the C/A and P codes by the same amount. Consequently, the receiver satellite distance will be too short if measured by the carrier phase and too long if measured by the code, compared with the actual distance. Ionospheric delay is proportional to the number of free electrons, called the Total Electron Content TEC, along the GPS signal path. TEC is used to calculate the effects of ionosphere on the GPS signal. It is number of electrons contained in unit area of 1m2 normal to the path of the radio signal under consideration. One unit of TEC called TECu is equivalent to 1016 electrons per m2. The value of 1 TECu for the L1 frequency generates a delay of 0.16 m. The ionosphere delay may be computed from [11]:

$$\Delta^{iono} = \frac{40.3}{f^2} . TEC \quad (3)$$

Where: Δ^{iono} is the ionosphere delay; f: wave frequency in MHz; and TEC: total electron content measured in TECu.

The factors that are affecting TEC are [12]:

1. The time of day, where electron density levels reach a daily maximum in early afternoon, and a minimum at midnight.
2. The time of the year, where electron density levels are higher in winter than in summer.
3. The 11-year solar cycle, where electron density levels reach a maximum value approximately every 11 years, which corresponds to a peak in the solar activities known as solar cycle peak.
4. The geographic location, where electron density levels are minimum in middle altitude regions, and these levels are maximum at polar and equatorial regions.

TEC is a fairly complicated quantity because it depends on sunspot activities, which is approximately 11-year cycle, seasonal and diurnal variations, the line of sight which includes elevation and azimuth of the satellite and the position of the observation site. The TEC may be measured, estimated, its effect computed by models, or eliminated. The integral is assumed to include the electrons in a column

ISSN 2229-5518

with a cross-section of 1m2 and extending from the receiver to the satellite [1].

3. Klobuchar Ionosphere Model

There are different ways to compute TEC, which allow correcting directly the single frequency observables. Many of them start from the Vertical Total Electron Content VTEC, which is sometimes denoted as total overhead electron content [13].

If VTEC is introduced in eq. (3), the quantities suffice only for satellites at zenith. For arbitrary line of sight, and with the assist of figure (1) which indicates single-layer model with the assumption that al1 free electrons are concentrated in an infinitesimally thick spherical shell at the height hm and containing the ionospheric point, the ionosphere delay may be written as [14]:

$$\Delta^{iono} = \frac{1}{\cos z'} \cdot \frac{40.3}{f^2} . VTEC \qquad (4)$$

$$\sin z' = \frac{R_E}{R_E + h_m} . \sin z_0 \qquad (5)$$

Where: RE is the mean radius of the earth, hm is a mean value for the height of the ionosphere which is ranging from 300 to 400km, and z' and z0 are the zenith angles at the ionospheric point IP and at the observing site respectively. The zenith angle z0 can be calculated for a known satellite position and approximate coordinates of the observation location.

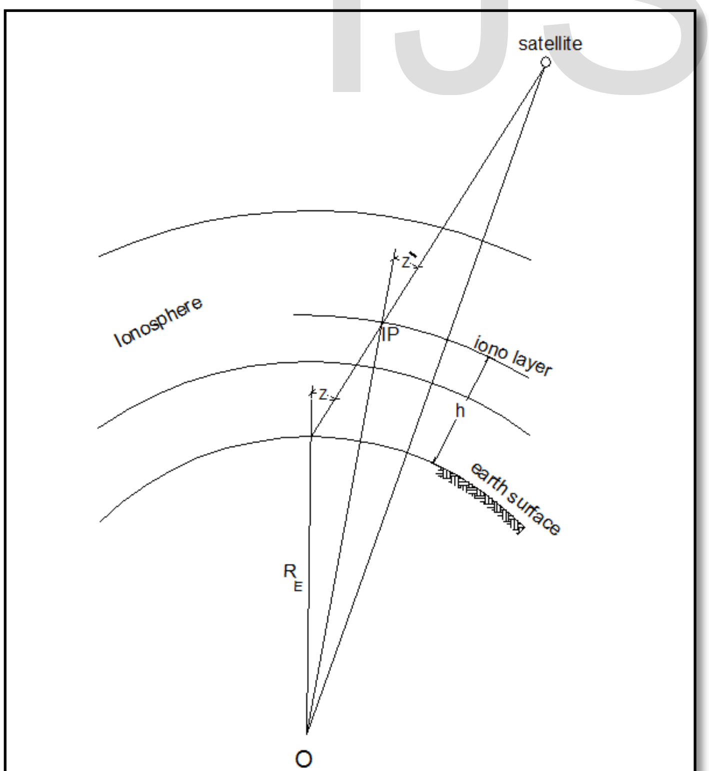

Fig. 1: Geometry of ionosphere delay (after Hofmann-Wellenhof, 2001)

Ionospheric Klobuchar model is adopted by single frequency GPS receivers to correct the ionospheric delay of the L1 carrier, developed around the mid-70s by J.A. Klobuchar. It is defined as a Single Layer Ionospheric model SLM, because the ionosphere is assumed to be concentrated in an infinitesimal layer placed at an average altitude of 350 km set by the Earth's surface. In a SLM the TEC is calculated in a geographic point called Ionospheric Point IP, which is obtained by the intersection between direction of propagation for ray path or line of sight, and the average height of the ionosphere [13].

Klobuchar model provides a different estimation for the daytime and night time ionospheric delay in seconds along the vertical direction, starting from eight coefficients, transmitted in the navigation message within the fourth sub frame of the navigation message. The delay is assumed to be constant at night time of a value of 5 nanoseconds, while is varying during the diurnal time. The Klobuchar model takes the following equation [1]:

$$\Delta_v^{iono} = A_1 + A_2 . \cos\left(\frac{2\pi(t - A_3)}{A_4}\right) \qquad (6)$$

Where: Δ_v^{iono} is the vertical ionosphere delay in seconds.

A1 =5 nanoseconds= 5x10-9 seconds.

$$A_2 = \alpha_1 + \alpha_2 . \emptyset_{IP}^{m} + \alpha_3 . \emptyset_{IP}^{m\,2} + \alpha_4 . \emptyset_{IP}^{m\,3} \qquad (7)$$

A3 = 14h local time.

$$A_4 = \beta_1 + \beta_2 . \emptyset_{IP}^{m} + \beta\alpha_3 . \emptyset_{IP}^{m\,2} + \beta_4 . \emptyset_{IP}^{m\,3}$$

$\propto_1$ to $\propto_4$ and β_1 to β_4 are broadcasted daily in the GPS satellites navigation message.

t is the local time of the ionospheric point IP and can be calculated from:

$$t = \frac{\lambda_{IP}}{15} + t_{ut} \qquad (8)$$

Where λ_{IP} is the geomagnetic longitude of the ionospheric point, and t_{ut} is the observation epoch in Universal Time.

ϕ_{IP}^{m} is the spherical distance between the geomagnetic pole and the ionospheric point IP, and can be calculated from:

$$\cos\phi_{IP}^{m} = \sin\phi_{IP} . \sin\phi_p + \cos\phi_{IP} . \cos\phi_p . \cos(\lambda_{Ip} - \lambda_p) \qquad (9)$$

ϕ_{Ip}, and λ_{Ip} are the latitude and longitude coordinates of the Ionospheric point.

$\phi_p = 78.3^o E$; and $\lambda_p = 291^0 N$ are the latitude and longitude coordinates of the geomagnetic pole

4. Global Ionospheric Models

Several organizations have been routinely providing ionospheric products to correct errors caused by the ionosphere in the form of ionospheric maps; in the shape of VTEC at grid points; including regional and global products, such as those from Wide Area Augmentation System WAAS and the International GNSS Service IGS, with various processing time delays ranging from near real time to a couple of weeks [15]. Among the earliest works of ionosphere modeling, the University of New Brunswick Ionospheric Modeling Technique UNB-IMT was developed in the mid-1990s. This technique was demonstrated to effectively derive both regional and global TEC maps. However, most of the models, including the current version of UNB-IMT, approximate the ionosphere using a single thin-shell approach with an altitude set at, for example 350 km, which may introduce additional modeling errors up to several TECu [16].

The IGS provides ionosphere VTEC values for a 50 x 50 global grid derived from a global network of monitoring stations equipped with dual frequency receivers. A rapidly growing globally distributed network of more than 150 dual-frequency GPS receivers currently exists and enables the monitoring of ionospheric TEC worldwide, with some notable gaps in the equatorial region and southern latitudes being filled. In addition to this GPS resource, the TEC data set can be augmented using other dual frequency tracking systems, such as the Doppler Orbitography and Radio positioning Integrated by Satellite DORIS and Precise Range And Range-Rate Equipment PRARE systems. By using spatial interpolation and temporal smoothing between the TEC measurements, combined with model information from a climatological ionospheric model, one may be able to produce Global Ionospheric Maps GIM of VTEC daily, hourly, or more frequently [15].

IGS has initiated a working group for the development of global ionospheric gridded data. The following analysis centres deliver their results of VTEC values in the IONospheric Exchange IONEX format which represents the ionosphere as an infinitesimal shell in time intervals of two hours [9]:

1. Centre for Orbit Determination in Europe CODE, University of Berne, Switzerland: Global Ionosphere Maps GIM are generated on a daily basis at CODE using data from about 150 GPS sites of the IGS and other institutions. The VTEC is modeled in a solar-geomagnetic reference frame using a spherical harmonics expansion up to degree and order 15. For the computation of the ionospheric pierce points, a spherical layer with a radius of 6821 km is assumed, implying geocentric latitudes.
2. Geodetic Survey Division of Natural Resources Canada known formerly as Energy, Mines and Resources Canada EMR, Ontario, Canada: The grid point values are mean VTECs estimated in a sun-fixed reference frame. The used observables are L1-L2 group delay with a carrier phase filtered.
3. European Space Operation Centre ESOC at the European Space Agency ESA, Darmstadt, Germany: The VTEC values are determined by vertical integration over Chapman Profile model using carrier phase leveled to code observables.
4. Jet Propulsion Laboratory JPL, Pasadena, USA: The VTEC is modeled in a solar-geomagnetic reference frame using bi-cubic splines on a spherical grid. A Kalman filter is used to solve simultaneously for instrumental biases and VTEC on the grid as stochastic parameters. The used observables are one-way carrier phase leveled to code.
5. Group of Astronomy and Geomatics, Universidad Politecnica da Catalunya GAG/UPC, Barcelona, Spain: The global ionosphere maps are modeled with a tomographic approach: two layers of cubic vowels with length of about 500 km in latitude, longitude and height. The height boundaries are 59, 739, and 1419 km. The estimates are interpolated with splines and radial basis functions. The used observables are phase differences L1-L2.

5. Description of the Field Test and Data Processing

The objective of this paper is to statically analyze the difference in 3-d coordinates resulted from processing GPS medium baselines up to 40 km, using Klobuchar, or CODE ionosphere correction model, or in case of not using any ionosphere models. The methodology of this paper will be based on comparing the 3-d Cartesian coordinates of 15 GPS baselines with approximate distances from 2 km to 40 km, which were processed using single frequency data L1 using Klobuchar, CODE, and No- ionosphere models.

The field test was conducted at Riyadh, Saudi Arabia, on 2nd, 3rd, 4th, and 5th Feb 2014. A dual frequency GPS receiver of Leica Viva was setup at a reference control point [17]. A second dual frequency receiver of the same type was set up sequentially on 15 control points of approximate distances from 2 km to 40 km, from the base station. The observational operating parameters were the same for the two receivers, which are: static mode, elevation angle 150, and 15 seconds rate of observations. The observational duration of each baseline was as follows: 30 minutes for the baselines up to 5km, with an increasing occupation time of 20 minutes for every 5km increasing in baseline length i.e. 50 minutes for baselines up to 10km; 70 minutes for baselines up to 15km, etc. The raw data of the GPS campaign were downloaded and archived for processing using Leica Geo Office software [18].

The CODE ionosphere files related to the same GPS observations times were downloaded from ftp://ftp.unibe.ch/aiub/CODE [19]. files COD17780.ION, COD17781.ION, COD17782.ION, and COD17783.ION were downloaded which represent GPS week number 1778 and days number 0, 1, 2, and 3 corresponding to Feb 2, 2014 to Feb 5, 2014 respectively.

ISSN 2229-5518

The 15 GPS baselines were processed using Leica Geo Office software three times using single frequency data L1. The first run was using Klobuchar ionosphere model; the second run was using CODE ionosphere model; and the last run was using No ionosphere model. The 3-d Cartesian coordinates for every run were archived for the statistical analysis.

6. Analysis of Results

The analysis of the results will be based on comparing the discrepancies in X, Y, Z coordinates, as well as positional discrepancy P between processing 15 GPS baselines using Klobuchar and CODE models, against processing the same baselines without any ionosphere model. Cartesian coordinate's discrepancies can be written as:

$$\Delta X_{klo-no} = X_{klo} - X_{no}$$
$$\Delta Y_{klo-no} = Y_{klo} - Y_{no} \quad (10)$$
$$\Delta Z_{klo-no} = Z_{klo} - Z_{no}$$

Where: ΔX_{klo-no} , ΔY_{klo-no} , and ΔZ_{klo-no} : the X, Y, and Z discrepancies between using Klobuchar model and No-ionosphere model.

X_{klo}, Y_{klo} , and Z_{klo} : the X, Y, and Z coordinates resulted from using Klobuchar model.

X_{no}, Y_{no} , and Z_{no} : the X, Y, and Z coordinates resulted from using No-ionosphere model.

The same set of equations no. 10 can be rewritten between CODE model and No-ionosphere model; aw well as between Klobuchar model and CODE model as follows:

$$\Delta X_{cod-no} = X_{cod} - X_{no}$$
$$\Delta Y_{cod-no} = Y_{cod} - Y_{no} \quad (11)$$
$$\Delta Z_{cod-no} = Z_{cod} - Z_{no}$$

Where: ΔX_{cod-no} , ΔY_{cod-no} , and ΔZ_{cod-no} : the X, Y, and Z discrepancies between using CODE model and No-ionosphere model.

X_{cod} , Y_{cod} , and Z_{cod} : the X, Y, and Z coordinates resulted from using CODE model.

$$\Delta X_{klo-cod} = X_{klo} - X_{cod}$$
$$\Delta Y_{klo-cod} = Y_{klo} - Y_{cod} \quad (12)$$
$$\Delta Z_{klo-cod} = Z_{klo} - Z_{cod}$$

Where: $\Delta X_{cod-cod}$, $\Delta Y_{cod-cod}$, and $\Delta Z_{cod-cod}$: the X, Y, and Z discrepancies between using Klobuchar model and CODE ionosphere model.

On the other hand, the positional discrepancies ΔP, and Standard Deviation σΔp for every pairs of solutions can be written as [20]:

$$\Delta P_{klo-no} = \sqrt{\Delta X^2_{klo-no} + \Delta Y^2_{klo-no} + \Delta Z^2_{klo-no}}$$
$$\Delta P_{cod-no} = \sqrt{\Delta X^2_{cod-no} + \Delta Y^2_{cod-no} + \Delta Z^2_{cod-no}} \quad (13)$$
$$\Delta P_{klo-cod} = \sqrt{\Delta X^2_{klo-cod} + \Delta Y^2_{klo-cod} + \Delta Z^2_{klo-cod}}$$

$$\sigma^2_{\Delta P_{klo-no}} = \sigma^2_{\Delta X_{klo-no}} + \sigma^2_{\Delta Y_{klo-no}} + \sigma^2_{\Delta Z_{klo-no}}$$
$$\sigma^2_{\Delta P_{cod-no}} = \sigma^2_{\Delta X_{cod-no}} + \sigma^2_{\Delta Y_{cod-no}} + \sigma^2_{\Delta Z_{cod-no}} \quad (14)$$
$$\sigma^2_{\Delta P_{klo-cod}} = \sigma^2_{\Delta X_{klo-cod}} + \sigma^2_{\Delta Y_{klo-cod}} + \sigma^2_{\Delta Z_{klo-cod}}$$

The discrepancies in X, Y, Z and position P, between processing the GPS data using Klobuchar and using No-ionosphere are shown in Table (1).

Table 1: The discrepancies in X, Y, Z, and position P between Klobuchar and No-ionosphere models

Baseline No.	Approx. Length (km)	Δ X (mm)	Δ Y (mm)	Δ Z (mm)	Δ P (mm)
1	2.2	0.5	1	-1.1	1.6
2	5.3	-0.9	0.4	-1.9	2.1
3	7.6	0.1	2.9	-1.9	3.5
4	10.2	1.2	-3.2	1.4	3.7
5	12.6	-2.1	3.4	2.1	4.5
6	15.9	-2.4	-4.8	-2	5.7
7	18.2	2.6	-6.4	3.1	7.6
8	20.5	-4	6.9	-2.8	8.5
9	22.8	-4.3	8.3	6.5	11.4
10	25.7	6.8	9.2	-6.1	13.0
11	27.4	-10.1	10.9	6.7	16.3
12	30.1	14.8	-13.7	-7.6	21.6
13	33.4	19.5	-17.5	-16.1	30.8
14	36.4	22.5	-17.4	23.4	36.8
15	40.3	-28.7	33.1	-27.8	51.9

The Cartesian coordinates X, Y, Z, and the Positional P discrepancies between using Klobuchar and No-ionosphere models are illustrated in Figures (2) and (3).

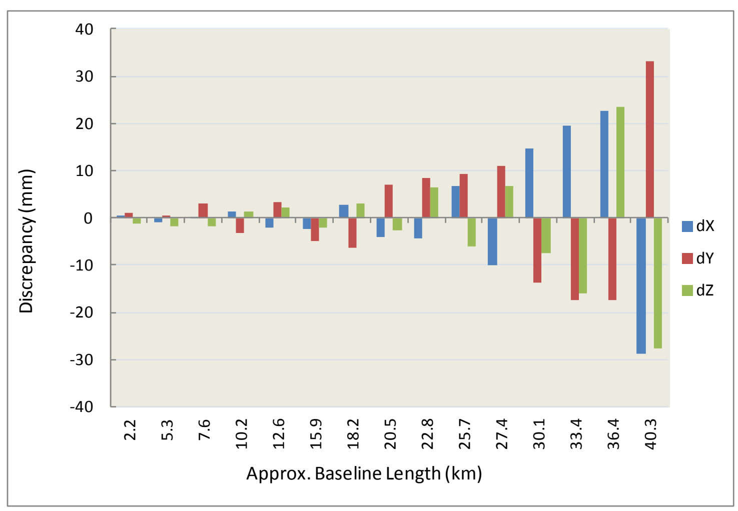

Fig. 2: Variation of the X, Y, and Z coordinate discrepancies between Klobuchar and No-ionosphere models

ISSN 2229-5518

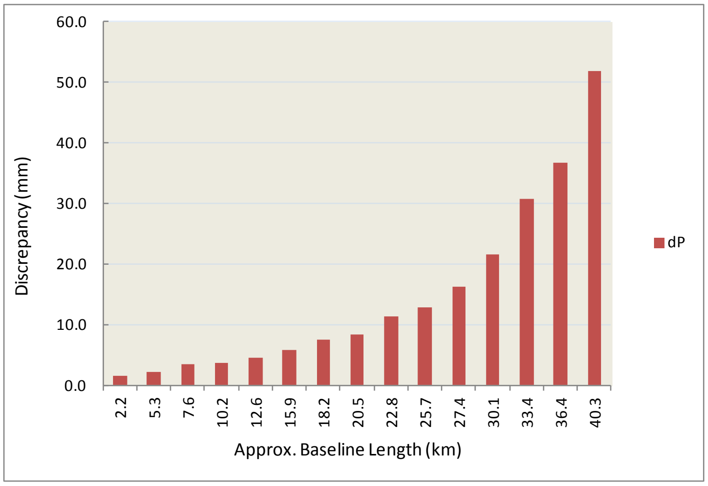

Fig. 3: Variation of the Positional Discrepancy P between Klobuchar and No-ionosphere models

The descriptive statistics of the above findings are tabulated in Table (2). For instance, the X-coordinate discrepancies are ranging between 22.5mm and -28.7mm, with mean value 1.0mm and SD 12.3mm for single determination. The Y-coordinate discrepancies are fluctuating between 33.1mm and -17.5mm, with mean value of 0.9mm and SD for single observation of 12.8mm. The Z-coordinate discrepancies are varying between 23.4mm and -27.8mm, with mean value of -1.6mm and SD for single determination of 11.2mmm. Finally, the positional discrepancies P between using Klobuchar and No-ionosphere models are differing from 1.6mm to 51.9mm, with most probable value of 14.6mm and SD 21.0mm respectively.

Table 2: Descriptive statistics of the discrepancies between Klobuchar and No-ionosphere models (mm)

Discrep.	Max.	Min.	Range	Mean	S.Dsingle	S.Dmean
ΔX	22.5	-28.7	51.2	1.0	12.3	3.2
ΔY	33.1	-17.5	50.6	0.9	12.8	3.3
ΔZ	23.4	-27.8	51.2	-1.6	11.2	2.9
ΔP	51.9	1.6	50.3	14.6	21.0	5.4

The previous set of tables and figures were created again between processing the GPS baseline CODE ionosphere and No-ionosphere models. The findings are tabulated in Tables (3), and (4) and Figures (4) and (5).

Table 3: The discrepancies in X, Y, Z, and position P between CODE and No-ionosphere models

Baseline No.	Approx. Length (km)	Δ X (mm)	Δ Y (mm)	Δ Z (mm)	Δ P (mm)
1	2.2	-0.7	0.2	2.0	2.1
2	5.3	0.3	2.0	-0.6	2.1
3	7.6	0.8	1.6	0.9	2.0
4	10.2	0.4	-0.6	-1.2	1.4
5	12.6	-1.7	-2.9	-0.9	3.5
6	15.9	-2.3	3.1	-1.7	4.2
7	18.2	3.9	-9.8	2.9	10.9
8	20.5	-3.6	9.8	3.9	11.1
9	22.8	4.0	13.1	7.6	15.7
10	25.7	7.7	19.3	-11.0	23.5
11	27.4	-7.2	16.5	15.2	23.6
12	30.1	14.5	-12.9	-13.8	23.8
13	33.4	19.0	-17.1	-19.5	32.2
14	36.4	29.7	-29.1	21.1	46.6
15	40.3	-29.1	27.3	-28.2	48.9

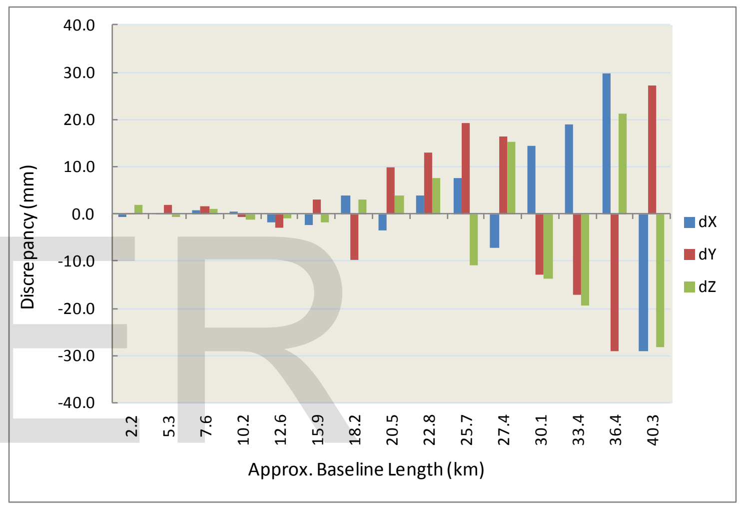

Fig. 4: Variation of the X, Y, and Z coordinate discrepancies between CODE and No-ionosphere models

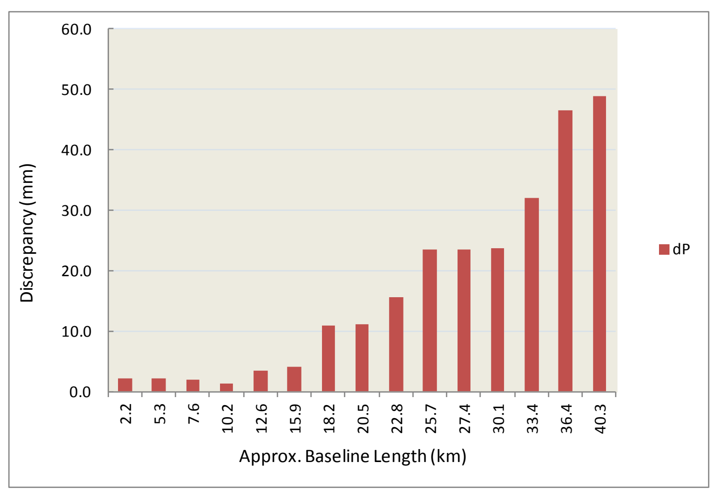

Fig. 5: Variation of the Positional Discrepancy P between CODE and No-ionosphere models

Table 4: Descriptive statistics of the discrepancies between CODE and No-ionosphere models (mm)

Discrep.	Max.	Min.	Range	Mean	S.Dsingle	S.Dmean
ΔX	29.7	-29.1	58.8	2.4	13.0	3.4
ΔY	27.3	-29.1	56.4	1.4	14.8	3.8
ΔZ	21.1	-28.2	49.3	-1.6	12.6	3.3
ΔP	48.9	1.4	47.5	16.8	23.4	6.0

For example, the positional discrepancy P between CODE and No-ionosphere models are ranging between 1.4 mm and 48.9mm with mean value of 16.8 mm and standard deviation of 23.4 mm for single determination.

The last set of tables and figures are describing the cartesian and positional discrepancies between processing the GPS data Klobuchar and CODE models. In this regard, the results are tabulated in Tables (5), and (6) and figures (6) and (7).

Table 5: The discrepancies in X, Y, Z, and position P between Klobuchar and CODE models

Baseline No.	Approx. Length (km)	Δ X (mm)	Δ Y (mm)	Δ Z (mm)	Δ P (mm)
1	2.2	-1.2	-0.8	3.1	3.4
2	5.3	1.2	1.6	1.3	2.4
3	7.6	0.7	-1.3	2.8	3.2
4	10.2	-0.8	2.6	-2.6	3.8
5	12.6	0.4	-6.3	-3.0	7.0
6	15.9	0.1	7.9	0.3	7.9
7	18.2	1.3	-3.4	-0.2	3.6
8	20.5	0.4	2.9	6.7	7.3
9	22.8	8.3	4.8	1.1	9.7
10	25.7	0.9	10.1	-4.9	11.3
11	27.4	2.9	5.6	8.5	10.6
12	30.1	-0.3	0.8	-6.2	6.3
13	33.4	-0.5	0.4	-3.4	3.5
14	36.4	7.2	-11.7	-2.3	13.9
15	40.3	-0.4	-5.8	-0.4	5.8

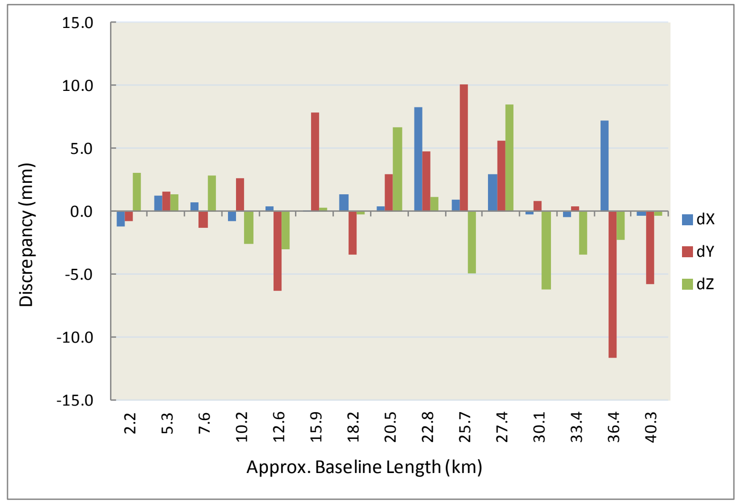

Fig. 6: Variation of the X, Y, and Z coordinate discrepancies between Klobuchar and CODE models

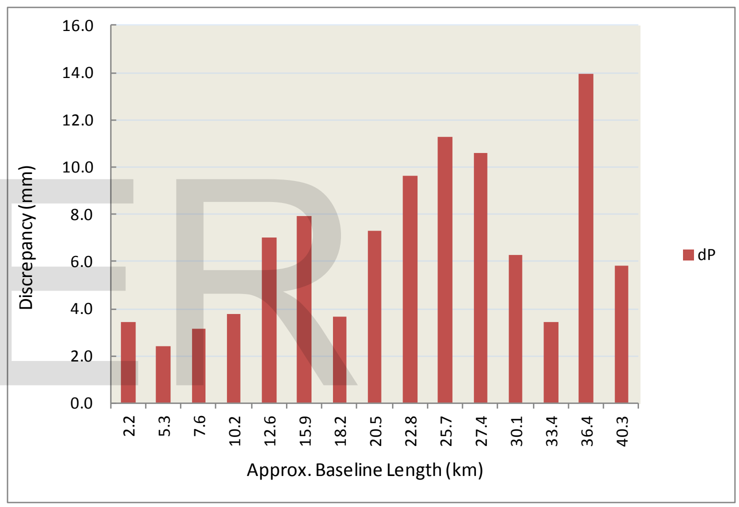

Fig. 7: Variation of the Positional Discrepancy P between Klobuchar and CODE models

Table 6: Descriptive statistics of the discrepancies between Klobuchar and CODE models (mm)

Discrep.	Max.	Min.	Range	Mean	S.Dsingle	S.Dmean
ΔX	ΔX	8.3	-1.2	9.5	1.3	2.8
ΔY	ΔY	10.1	-11.7	21.8	0.5	5.7
ΔZ	ΔZ	8.5	-6.2	14.7	0.1	4.1
ΔP	ΔP	13.9	2.4	11.5	6.6	7.6

For example, the positional discrepancy P between Klobuchar and CODE models are ranging between 2.4mm and 13.9 mm with mean value of 6.6mm and standard deviation of 7.6mm for single determination.

Finally, the positional discrepancies between each pair of ionosphere models i.e. Klobuchar Vs No-ionosphere, CODE

ISSN 2229-5518

Vs No-ionosphere, and Klobuchar Vs CODE are displayed in figure (8).

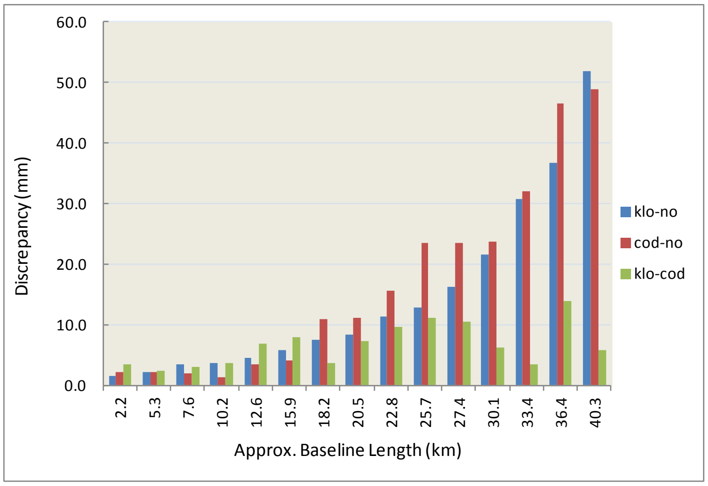

Fig. 8: Positional discrepancies between Klobuchar, CODE, and No-ionosphere models

7. CONCLUSIONS

The present study discusses the effect of using different ionosphere models on the resulted Cartesian coordinates resulted from processing GPS medium baselines up to 40km. A GPS campaign was conducted to observe 15 baselines varying from 2km to 40km. The GPS single frequency data were processed using: Klobuchar, CODE correction model from university of Berne, and using No-ionosphere model. The Cartesian coordinates resulted from using Klobuchar and CODE models were compared with the resulted cartesian coordinates from using No-Troposphere model.

The statistical analysis of the obtained results showed the following:

1. The discrepancies in X, Y, and Z coordinates between using Klobuchar model and using No-ionosphere model have mean values of 1.0mm, 0.9mm, and -1.6mm respectively. The standard deviations for the previous findings are 3.2mm, 3.3mm, and 2.9mm respectively.
2. The discrepancies in X, Y, and Z coordinates between using CODE correction model and using No-ionosphere model have mean values of 2.4mm, 1.4mm, and -1.6mm. The standard deviations for the previous values are 3.4mm, 3.8mm, and 3.3mm respectively.
3. The discrepancies in X, Y, and Z coordinates between using Klobuchar and CODE correction models have mean values of 1.3mm, 0.5mm, and 0.1mm. The standard deviations for the previous values are 0.7mm, 1.5mm, and 1.1mm respectively.
4. The positional discrepancies between Klobuchar model and No-ionosphere has a mean value of 14.6mm and 5.4mm standard deviation; while the positional discrepancy between CODE model and No-ionosphere model has a mean value of 16.8mm with 6.0mm standard deviation. Finally, the positional discrepancy between Klobuchar and CODE models has a mean value of 6.6mm with 2.0mm standard deviation, which means that both Klobuchar and CODE models are giving almost the same results.

The previous results showed that there are no significant differences in the resulted cartesian coordinates in case of processing GPS single frequency baselines collected with static technique, using Klobuchar or CODE ionosphere models, or in case of processing data without any ionosphere models. These findings may be adopted for establishing first order geodetic networks up to 40km baseline lengths with less-expensive GPS single frequency receivers. On the other hand, in case of using GPS single frequency receivers in monitoring the deformation of structures, it is recommended to use the same ionosphere model in comparing monitoring results, to maintain the millimeter accuracy.

8. REFERENCES

1. Hofmann-Wellenhof B., H. Lichtenegger and J. Collins (2001): "Global Positioning System, Theory and Practice", 5th Revised Edition, Springer-Verlag, New York.
2. Kaplan E. (1996): "Understanding GPS, Principles and Applications", Norwood, MA, Artech House.
3. Rizos C. (1997): "Principles and Practice of GPS Surveying", Monograph 17, School of Geomatics Engineering, the University of New South Wales.
4. Seeber G. (1993): "Satellite Geodesy, Foundations, Methods and Applications", Walter de Gruyter, Berlin.
5. Abdel Mageed Kh. (2006): "Towards improving the accuracy of GPS single point positioning", Ph.D Thesis, Faculty of Engineering, Department of Public Works, Ain Shams University, Cairo, Egypt.
6. Leick A. (1995): "GPS Satellite Surveying", A Willey Inter-Science Publications, John Willey & Sons, New York.
7. Abdel Mageed Kh. (2011): "Accuracy assessment for processing GPS short baselines using ionosphere-free linear combination", Australian Journal of Basic and Applied Sciences, vol. 5, no. 9.
8. Klobuchar J. A. (1991): "Ionospheric Effects on GPS", GPS World, vol. 2, no. 4.

ISSN 2229-5518

9. International GNSS Service IGS (2012): "IGS Technical Report". ftp://igs.org/pub/resource/pubs/2012_techreport.pdf.
10. El-Rabbany A. (2002): "Introduction to the Global Positioning System GPS", Artech House Mobile Communications Series, Boston, London.
11. Guochang Xu (2007): "GPS Theory, Algorithms, and Applications", Second Edition, Springer Publishing, New York.
12. Grant D. B., C. Rizos, and A. Stolz (1990): "Dealing with GPS Biases, some Theoretical and Software Considerations", School of Surveying, University of New South Wales, Australia.
13. Cohen C. E., B. Pervan, and B. W. Parkinson (1992): "Estimation of absolute ionospheric delay exclusively through single-frequency GPS measurements", ION-GPS Meeting, Albuquerque.
14. Klobuchar J. A. (1987): "Ionospheric time-delay algorithm for single-frequency GPS users", IEEE Transactions on aerospace and electronic systems, vol. 23, no. 3.
15. Feltens J., Angling M., Jakowski N., Mernandez-Pajares M., and Zandbergen R. (2010): "GNSS contribution to next generation global ionospheric monitoring", Beacon Satellite Symposium, Barcelona.
16. Feltens J. (2007): "Development of a new three-dimensional mathematical ionosphere model at European Space Agency/European Space Operations Centre", Space Weather – The International Journal of Research and Applications, vol. 5, no. 12.
17. Leica Company (2012): "Leica Viva GNSS, Technical Reference Manual", www.leica-geosystems.com
18. Leica Company (2012): "Leica Geo Office Combined, Online Help", www.leica-geosystems.com
19. Center for Orbit Determination in Europe CODE (2014): "Global ionosphere maps produced by CODE", ftp://ftp.unibe.ch/aiub/CODE.
20. Comery A., P. Bott, and H. Lee (1989): "Elementary Statistics, A Problem-Solving Approach", WM. C. Brown Publishers, California, USA.